JACS
JOURNAL OF THE AMERICAN CHEMICAL SOCIETY

ARTICLE

pubs.acs.org/JACS

Three-Dimensional Nanocrystal Superlattices Grown in Nanoliter Microfluidic Plugs

Maryna I. Bodnarchuk, Liang Li, Alice Fok, Sigrid Nachtergaele, Rustem F. Ismagilov, and Dmitri V. Talapin*

Department of Chemistry, University of Chicago, Chicago, Illinois 60637, United States

Supporting Information

ABSTRACT: We studied the self-assembly of inorganic nanocrystals (NCs) confined inside nanoliter droplets (plugs) into long-range ordered superlattices. We showed that a capillary microfluidic platform can be used for the optimization of growth conditions for NC superlattices and can provide insights into the kinetics of the NC assembly process. The utility of our approach was demonstrated by growing large (up to 200 μm) three-dimensional (3D) superlattices of various NCs, including Au, PbS, CdSe, and $CoFe_2O_4$. We also showed that it is possible to grow 3D binary nanoparticle superlattices in the microfluidic plugs.

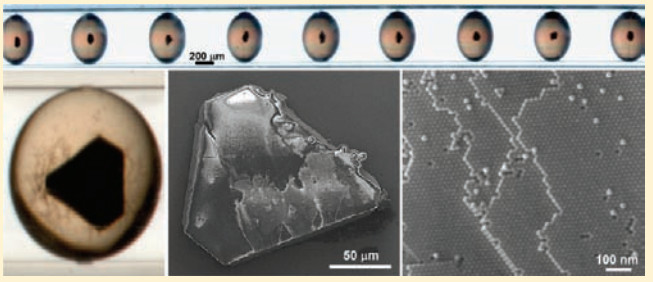

1. INTRODUCTION

Many key features of ordinary crystals (e.g, faceting, twinning, polymorphism, etc.) have been observed in nanocrystal (NC) superlattices, suggesting that their assembly follows the same fundamental principles as crystallization of conventional atomic and molecular solids.[1−4] In contrast to individual atoms and molecules, which are very difficult to image in real space, NCs provide a unique chance to study the crystallization of complex structures in real space and real time. Such studies should provide important insights into the fundamental aspects of crystal nucleation and growth, formation of structural defects, etc.[5] Control over the formation of ordered single-component[2,6−8] and binary[9−15] NC arrays is also important for successful development of NC-based electronic and optoelectronic devices such as solar cells, photodetectors, field-effect transistors, and light-emitting diodes.[16]

The approaches to growing NC superlattices can be divided in two categories. In "evaporation-driven" methods, the carrier solvent is slowly evaporated from a colloidal solution of NCs.[8,9,12−14] When the NC volume fraction reaches a certain threshold, the system undergoes a transition from a disordered state to an ordered one.[17] In contrast, "destabilization-driven" approaches use slow destabilization of a colloidal solution, which is typically achieved by layering the NC solution with a precipitant that slowly diffuses into the NC solution. This approach is similar to the technique of free interface diffusion used in protein crystallization.[18] It allows the growth of large three-dimensional (3D) faceted crystals of long-range-ordered NCs.[4,6,19−22]

Like many other crystallization experiments, NC assembly requires numerous trials to find the optimal conditions, especially in the case of binary nanoparticle superlattices (BNSLs). The availability of techniques for fast combinatorial screening of experimental parameters would greatly accelerate such studies. In protein research, high-throughput crystallization studies often employ robotics[23] and microfluidics.[24−27] The latter case provides a number of unique advantages, such as ultrasmall materials consumption and precise control over molecular diffusion and crystal nucleation.[18]

In this work, we applied a microfluidic platform for studies of the self-assembly of colloidal NCs. It allowed us to explore the homogeneous nucleation and support-free growth of NC superlattices with fast combinatorial screening of the experimental conditions.

2. EXPERIMENTAL DETAILS

Figure 1a and Figure S1 in the Supporting Information (SI) show our experimental setup for the formation of nanoliter droplets confined inside a microfluidic capillary. The capillary (thin-wall Teflon tubing) was cut and inserted into lithographically defined polydimethylsiloxane (PDMS) devices. The NC solution and precipitant were simultaneously injected into a stream of immiscible fluorinated carrier fluid (Figure 1a and Figure S1). The injection rates were synchronized by a LabView program controlling several syringe pumps. The width of the plugs was determined by the inner diameter of the capillary (400 μm), while the plug volume could be varied by tuning the flow rates of the solutions entering the capillary, with reproducibility of the plug volumes within 3−20%.[28] The separation between plugs was controlled by the flow rate of the carrier fluid.

As the carrier fluid, we used a mixture of perfluoro-tri-*n*-butylamine and perfluoro-di-*n*-butylmethylamine (FC-40) or perfluorotripentylamine (FC-70). These fluids showed the lowest miscibility with alcohols and toluene.[29] FC-40 and FC-70 have high boiling points (155 and 215 °C, respectively) and preferentially wet the surface of the Teflon capillary. The latter allowed us to minimize the contact area between the

Received: February 5, 2011
Published: April 21, 2011

dx.doi.org/10.1021/ja201129n | J. Am. Chem. Soc. 2011, 133, 8956–8960

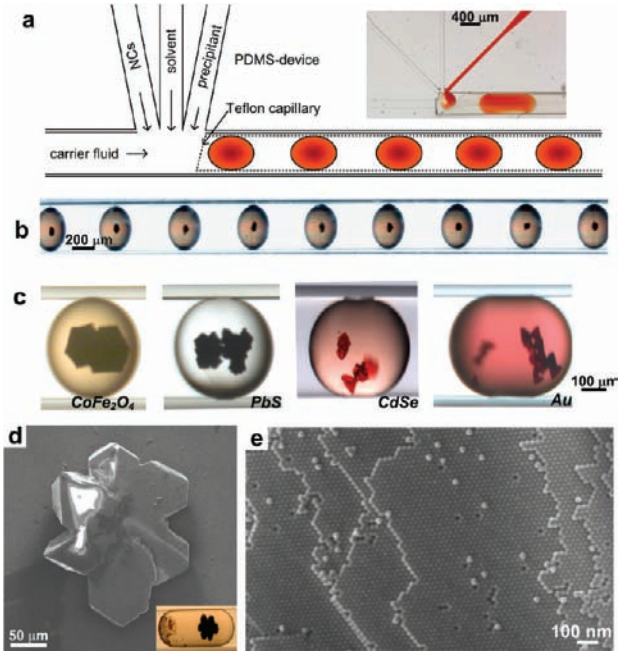

Figure 1. (a) Microfluidic device used for NC self-assembly. The nanoliter plugs were formed by mixing the NC colloidal solution with the precipitant. The inset shows an optical photograph of a typical PDMS device during an experiment. (b) Optical image of an array of plugs containing PbS NC superlattices. (c) Optical images of plugs containing superlattices formed from various NCs: 11 nm $CoFe_2O_4$, 10 nm PbS, 3.5 nm CdSe, and 7 nm Au (left to right). (d) SEM image of a faceted superlattice of 11 nm $CoFe_2O_4$ NCs grown by incubation of plugs containing NCs in the ethanol/toluene solution. The inset shows an optical image of the plug containing exactly the same superlattice. (e) High-resolution SEM image of a superlattice self-assembled from 20 nm $CoFe_2O_4$ NCs.

plugs and the capillary walls. The plugs were injected directly into the Teflon capillary (Figure 1a and Figure S1) to minimize the contact of PDMS with toluene and prevent PDMS swelling.[30] To further suppress swelling, PDMS channels were treated with silane and covered with Teflon using a fluoropolymer solution.[31,32]

In this work, we used magnetic ($CoFe_2O_4$),[33] semiconducting (CdSe and PbS),[34] and metallic (Au and Pd) NCs synthesized by colloidal chemistry techniques. Before carrying out the microfluidic experiments, we confirmed the ability of all of the NC samples to form superlattices using conventional evaporation-driven and destabilization-driven methods.

Two modes of superlattice growth were used to mimic the destabilization-driven and evaporation-driven approaches. In the former case, the NCs, solvent, and precipitant were combined in each plug. In the latter experiments, solutions of NCs in toluene or tetrachloroethylene (TCE) were introduced into plugs without the addition of a precipitant. Over time, toluene and TCE slowly diffused into the carrier fluid and evaporated through the walls of the Teflon capillary, leading to a gradual reduction of the plug volume up to complete solvent evaporation. We noticed extremely small amounts of sample consumption during the microfluidic experiments, typically 30−50 μL of colloidal solution per 1000 plugs.

3. RESULTS AND DISCUSSION

Destabilization-Driven Self-Assembly of NCs in Microfluidic Plugs. To generate plugs containing different precipitant/toluene ratios, we systematically varied the relative flow rates of solvent and precipitant (Figure 1a). Previous studies with dye molecules added for in situ concentration measurements confirmed the accuracy of such concentration tuning.[27,29] Short-chain alcohols such as ethanol, isopropanol, and *n*-butanol were found to be suitable precipitants. To minimize solvent evaporation through the Teflon walls, the capillary was placed inside a 3 mm diameter glass tube filled with FC-70 and sealed with wax at both ends (Figure S2). The samples were then incubated for 5−10 days until the initially strongly colored plugs turned into nearly colorless solutions containing one or several 3D superlattices (Figure 1b,c).

Superlattices typically nucleated in the bulk of solution close to the center of the plug (Figure 1b,c). However, in the case of 20 nm $CoFe_2O_4$ NCs, we observed nucleation at the interface with the carrier fluid when ethanol was used as the precipitant, while nucleation occurred in the bulk solution when isopropanol was used to destabilize a colloidal solution of the same NCs (Figure S3).

The typical dimensions of the 3D superlattices ranged from a few to several hundred micrometers, comparable to the largest reported NC superlattices obtained by colloidal crystallization in test tubes.[4,6,19−22] Proper tuning of the precipitant/solvent ratio allowed an impressive plug-to-plug reproducibility of the crystallization conditions, as demonstrated in Figure 1b, where only one PbS NC superlattice nucleated and grew in the center of each plug.

To illustrate the generality of this approach, we prepared superlattices from Au, CdSe, PbS, and $CoFe_2O_4$ NCs of various sizes (Figure 1c and Figure S4). Low-magnification scanning electron microscopy (SEM) images showed well-defined superlattice facets (Figure 1d and Figure S4). A survey of high-resolution SEM images revealed characteristic low-index projections of a face-centered cubic (fcc) lattice (Figure S5) with clearly resolved surface terraces, steps, vacancies, "adatom" ledges, and kinks (Figure 1e and Figure S5). All of these features were analogous to those expected for fcc crystals in the terrace−ledge−kink model of Burton, Cabrera, and Frank.[35] Many superlattices contained twin planes, which was rather expected because of the low twinning energy in fcc NC superlattices.[4] Some superlattices also showed screw dislocations (Figure S5b), which could play an important role in the nucleation and growth of free-standing NC superlattices in a way similar to the nucleation and growth of ordinary crystals from a screw dislocation.[36]

To find the conditions leading to large NC superlattices with well-developed facets and few structural defects (e.g., Figure 1d and Figure S6), we systematically screened the precipitant/solvent ratio in the plugs. Figure 2a shows an example of ethanol/toluene ratio screening for 10 nm PbS NCs. The concentration of ethanol in the plugs was continuously increased from 10 to 40% (Figure S7d), while the concentration of NCs was kept constant at $\sim 2 \times 10^{15}$ NCs/mL. At particular ethanol/toluene ratios, we observed sharp transitions from plugs containing only NC colloid to plugs with crystals surrounded by solution and then to plugs with a disordered precipitate.

The conditions for NC self-assembly could be further refined by using precipitants with different polarities (Figure 2b and Figure S7). As an example, we compared the destabilization of toluene solutions of 11 nm $CoFe_2O_4$ NCs ($\sim 1 \times 10^{15}$ NCs/mL) by ethanol, isopropanol, and *n*-butanol with systematic variation of the alcohol/toluene volume ratio from 10 to 80%. The destabilization of NC colloids occurred almost immediately when the concentration of ethanol in the plug was in the range

dx.doi.org/10.1021/ja201129n |J. Am. Chem. Soc. 2011, 133, 8956–8960

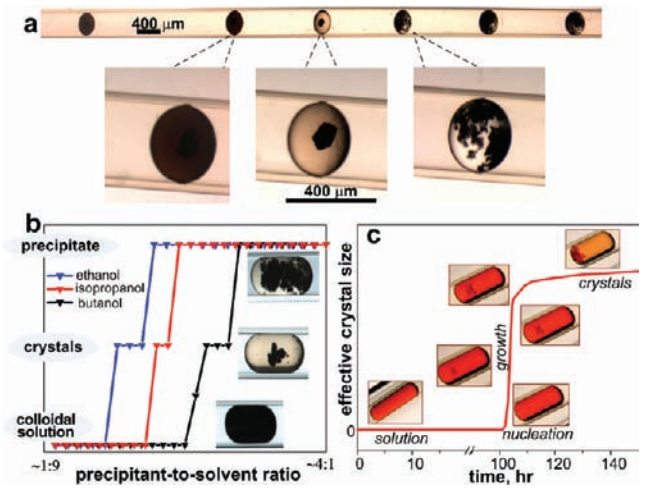

Figure 2. (a) Systematic screening of the precipitant/solvent ratio in the microfluidic plugs. A solution of 10 nm PbS NCs in toluene was mixed with ethanol. The ethanol concentration was systematically increased from ~10 to 40%. As the toluene concentration decreased, we observed a transition from plugs with clear NC solutions to plugs containing large NC superlattices to plugs with disordered precipitate. (b) "Phase diagrams" for self-assembly of 11 nm $CoFe_2O_4$ NCs in an array containing 26 microfluidic plugs. Depending on the polarity of the precipitant, the transitions from plugs with solution to those with superlattices to those with precipitate were observed at different precipitant/toluene ratios (see the text for further details). (c) Kinetic study showing the nucleation and growth of 3 nm CdSe NC superlattices in a microfluidic plug containing toluene and ethanol as the solvent and precipitant, respectively.

from ~25 to 80% (Figure 2b). In the case of *n*-butanol, fast destabilization of the colloidal solutions was observed in plugs containing ~65−80% alcohol. The crystal growth occurred rapidly in the presence of ethanol and much more slowly in the presence of *n*-butanol. The first crystals appeared in 1 day in ethanol/toluene plugs and 3 days in butanol/toluene plugs. Isopropanol showed behavior intermediate between those of ethanol and *n*-butanol. Generally, the use of a less-polar precipitant such as *n*-butanol resulted in a broader window of concentrations suitable for self-assembly of high-quality NC superlattices because of gentler destabilization of the colloidal solutions. We also noticed high reproducibility of the crystallization experiments. For example, Figure S8 shows the results of four experiments where the *n*-butanol concentration was systematically varied from 20 to 80 vol %. In all cases, large superlattices formed in the plugs at identical precipitant/solvent ratios.

Kinetics of Homogeneous Superlattice Nucleation in Nanoliter Droplets. The microfluidic plugs can be used to study the kinetics of colloidal crystallization, which is hardly accessible in conventional experiments. In the case of 3 nm CdSe NCs, the transparency of the colloidal solution permitted easy monitoring of the nucleation and growth of NC superlattices in individual plugs by simple optical microscopy (Figure 2c). We generated plugs with high concentrations of CdSe NCs (~10^{17} NCs/mL) and a 1:4 ethanol/toluene ratio and monitored their evolution by taking micrographs every 15 min. No precipitation was observed during the first 4 days. During this time, the plug volume decreased by ~25% because of slow evaporation of toluene (which is much more soluble in FC-40 and FC-70 than ethanol[29]) through the walls of the Teflon tubing (Figure 2c). After 103 h, the concentration of NCs reached the nucleation threshold, and we observed the sudden appearance of red crystals. These crystals quickly grew to their near-final size within 1 h (Figure 2c and Figure S9; also see the video clip in the SI). The fast growth was followed by continuous, very slow growth of NC superlattices over the next 2 days. Finally, discoloration of the colloidal solution evidenced the completion of NC superlattice formation. Very similar kinetics was observed in other plugs with the same ethanol/toluene ratio (Figure S10).

In contrast to conventional test tube experiments based on the interdiffusion of solvent and precipitant layers,[4,6,19−22] the precipitant/solvent ratio in microfluidic plugs was established almost immediately during formation of the plug. Any spatial variations of composition promptly equilibrated as the plug moved through the capillary.[37] Diffusion of toluene out of the plugs resulted in a slow but continuous increase of the ethanol/toluene ratio. The observation of steplike growth kinetics shows that homogeneous nucleation of an NC superlattice is preceded by strong supersaturation of the colloidal solution. Right after the nucleation event, the fast growth of superlattices was controlled by diffusion of NCs inside the plug. This fast growth proceeded until the chemical potential of the superlattice became equal to the chemical potential of the colloidal solution. The slow kinetics of further superlattice growth was probably governed by slow diffusion of toluene out of the plug.

Evaporation-Driven Self-Assembly of NCs in Microfluidic Plugs. When no precipitant was added to a plug containing a colloidal solution of NCs, the crystallization threshold was approached by slow evaporation of solvent through the microporous walls of the thin-walled Teflon tubing when samples were left under open air without the extra glass tubing (Figure 3a). Typically, toluene evaporated from 130−150 nL plugs containing 10^{14}−10^{15} NCs/mL at a rate of ~1 nL/h. The plug volume gradually decreased, with complete evaporation of the solvent occurring after 5−6 days. In contrast to commonly used solvent evaporation on transmission electron microscopy (TEM) grids, the plug evaporation occurred in the absence of a solid substrate.

A low-resolution SEM image (Figure 3b) showed round-shaped precipitates. This was strikingly different from destabilization-driven assembly, which always produced faceted crystals. Close inspection of the round assemblies by SEM revealed that nearly all of the NCs were packed into long-range-ordered superlattices (Figure S11).

Formation of Binary NC Superlattices in Microfluidic Plugs. By combining two kinds of NCs, we attempted to grow BNSLs in microfluidic plugs using both the destabilization-driven and evaporation-driven approaches. Various combinations of 4 nm Pd, 7 nm Au, 8 nm CdSe, and 10 nm PbS NCs with 11 and 20 nm $CoFe_2O_4$ NCs were prepared and studied at various NC concentration ratios (1:2 to 1:10).

In the destabilization-driven experiments, we extensively screened combinations of a precipitant (ethanol, isopropanol, or butanol) with toluene or TCE. No BNSL structures were found in any of the studied samples. Instead, we reproducibly observed macroscopic phase separation of the NCs into fcc-packed individual components. For example, the mixture of 20 nm $CoFe_2O_4$ NCs and 10 nm PbS NCs crystallized into well-faceted, phase-separated fcc superlattices (Figure 3c and Figure S12).

The formation of BNSLs was observed in the evaporation-driven experiments when TCE was used as the solvent for the colloidal NCs. Figure 3d shows a fragment of a 3D BNSL formed

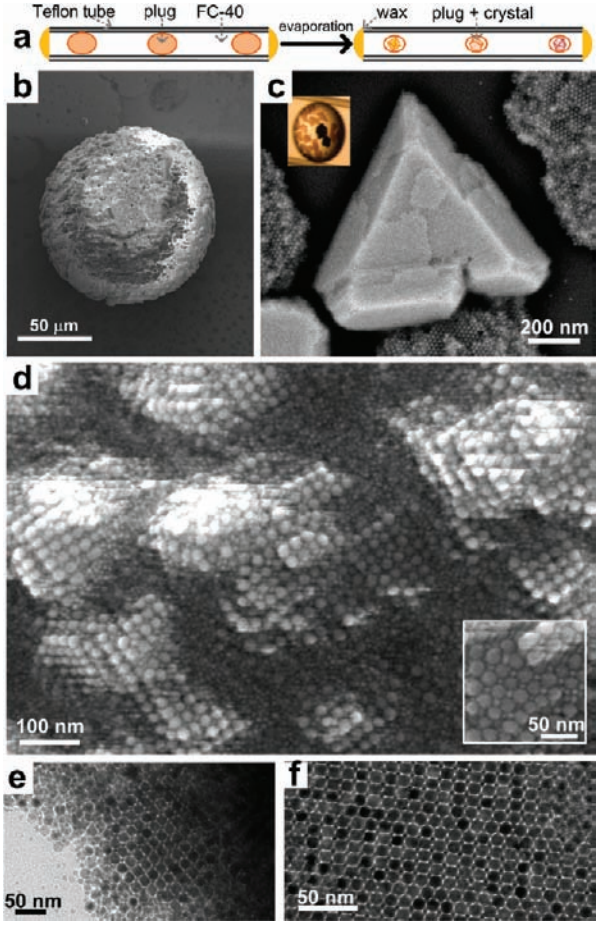

Figure 3. (a) Schematic illustration of evaporation-driven NC assembly in microfluidic plugs. (b) SEM image of an NC plug after complete solvent evaporation. (c) SEM image of phase-separated fcc superlattices formed in a plug containing a mixture of 20 nm $CoFe_2O_4$ NCs and 10 nm PbS NCs. Toluene and isopropanol were used as the solvent and precipitant, respectively. The inset shows a photograph of a plug containing two single-component superlattices assembled from $CoFe_2O_4$ NCs (brown) and PbS NCs (black). (d) SEM images of 3D AlB_2-type binary superlattices grown in plugs containing 20 nm $CoFe_2O_4$ NCs and 8 nm CdSe NCs. (e, f) TEM images of BNSL fragments prepared by the evaporation-driven method (e) in a plug and (f) on a TEM grid.

in a plug containing a mixture of 20 nm $CoFe_2O_4$ NCs and 8 nm CdSe NCs. To the best of our knowledge, this is the first observation of large 3D BNSLs.

The BNSL projection shown in Figure 3d could belong to one of several lattices [e.g., CuAu(001), AlB_2(110), or CsCl (001)].[9] To make a further structural assignment, we gently sonicated the BNSLs in ethanol and studied the obtained small fragments using TEM. Figure 3e shows a fragment that was assigned to the (110) projection of the AlB_2 lattice. In the control experiment, we slowly evaporated a solution of 20 nm $CoFe_2O_4$ NCs and 8 nm CdSe NCs in TCE using a TEM grid as a substrate and also observed the formation of AlB_2-type BNSLs (Figure 3f and Figure S13). The effective NC size ratio of 0.48 was calculated taking into account the thickness of the ligand shells.[12] This size ratio corresponded to the stability region for the AlB_2 phase.[38]

The differences in the outcomes for the destabilization-driven and evaporation-driven approaches could have their origin in the thermodynamics of the NC self-assembly process. Spontaneous assembly of NCs from a disordered state (colloidal solution) to the ordered state (superlattice) leads to minimization of the Helmholtz free energy $F = U - TS$. Previous studies have shown that the internal energy (U) is dominant when different types of NCs have opposite electrical charges[39] or when there is a large contrast in the van der Waals forces between the large and small NCs.[40] The latter case is typical when dielectric NCs (e.g., CdSe, PbS, or $CoFe_2O_4$) coassemble with metallic NCs (e.g., Au, Ag, Pd, etc).[12,13,15] In the other cases, the entropic term (TS) is the major driving force for BNSL formation.[10,14,15] The entropy alone can drive self-assembly of spherical particles only in very concentrated solutions where NCs occupy about half of the total solution volume.[17] Such conditions can be realized only during evaporation-driven assembly.

In the destabilization-driven process, the NC volume fraction in solution remains small, thus minimizing the effect of entropy, while the concentration of the precipitant determines the attractive potentials between hydrocarbon ligands at the NC surface. In this regard, destabilization-driven assembly is a U-driven process. If more than one type of particle is present in the solution, stepwise destabilization of the colloid occurs, starting with NCs exhibiting the strongest van der Waals forces. This effect is widely used for size-selective fractionation of polydisperse colloidal solutions.[40]

4. SUMMARY

Our study has demonstrated the utility of microfluidic techniques for self-assembly of colloidal NCs. The developed approach offers fast combinatorial screening of the crystallization conditions with very low materials consumption. We successfully grew large superlattices from metallic, semiconducting, and magnetic NCs as well as large 3D BNSLs. Further development of microfluidic platforms for NC assembly will open up many new opportunities, such as the control of surface chemistry to guide NC nucleation[41,42] and directed assembly of NCs under external electric and magnetic fields.

■ ASSOCIATED CONTENT

Ⓢ Supporting Information. Additional experimental details, SEM and optical images, and a video clip (AVI). This material is available free of charge via the Internet at http://pubs.acs.org.

■ AUTHOR INFORMATION

Corresponding Author
dvtalapin@uchicago.edu

■ ACKNOWLEDGMENT

We thank M. V. Kovalenko and S. Rupich for stimulating discussions and samples of CdSe and PbS NCs. This work was partially supported by the Office of Naval Research under Award N00014-10-1-0190. The collaborative work used the Chicago MRSEC Microfluidic Facility and was supported in part by the Chicago MRSEC funded by the NSF under Award DMR-0213745. D.V.T. thanks the David and Lucile Packard Foundation. R.F.I. and D.V.T. also acknowledge support from the Camille Dreyfus Teacher-Scholar Program.

REFERENCES

(1) Whetten, R. L.; Shafigullin, M. N.; Khoury, J. T.; Schaaff, T. G.; Vezmar, I.; Alvarez, M. M.; Wilkinson, A. *Acc. Chem. Res.* **1999**, *32*, 397.

(2) Murray, C. B.; Kagan, C. R.; Bawendi, M. G. *Science* **1995**, *270*, 1335.

(3) Bishop, K. J. M.; Wilmer, C. E.; Soh, S.; Grzybowski, B. A. *Small* **2009**, *5*, 1600.

(4) Rupich, S. M.; Shevchenko, E. V.; Bodnarchuk, M. I.; Lee, B.; Talapin, D. V. *J. Am. Chem. Soc.* **2009**, *132*, 289.

(5) Wang, Z. L. *Adv. Mater.* **1998**, *10*, 13.

(6) Murray, C. B.; Kagan, C. R.; Bawendi, M. G. *Annu. Rev. Mater. Sci.* **2000**, *30*, 545.

(7) Bigioni, T. P.; Lin, X. M.; Nguyen, T. T.; Corwin, E. I.; Witten, T. A.; Jaeger, H. M. *Nat. Mater.* **2006**, *5*, 265.

(8) Bodnarchuk, M. I.; Kovalenko, M. V.; Pichler, S.; Fritz-Popovski, G.; Hesser, G.; Heiss, W. *ACS Nano* **2010**, *4*, 423.

(9) Smith, D. K.; Goodfellow, B.; Smilgies, D. M.; Korgel, B. A. *J. Am. Chem. Soc.* **2009**, *131*, 3281.

(10) Chen, Z.; O'Brien, S. *ACS Nano* **2008**, *2*, 1219.

(11) Chen, J.; Ye, X. C.; Murray, C. B. *ACS Nano* **2010**, *4*, 2374.

(12) Shevchenko, E. V.; Talapin, D. V.; Murray, C. B.; O'Brien, S. *J. Am. Chem. Soc.* **2006**, *128*, 3620.

(13) Shevchenko, E. V.; Talapin, D. V.; Kotov, N. A.; O'Brien, S.; Murray, C. B. *Nature* **2006**, *439*, 55.

(14) Friedrich, H.; Gommes, C. J.; Overgaag, K.; Meeldijk, J. D.; Evers, W. H.; de Nijs, B.; Boneschanscher, M. P.; de Jongh, P. E.; Verkleij, A. J.; de Jong, K. P.; van Blaaderen, A.; Vanmaekelbergh, D. *Nano Lett.* **2009**, *9*, 2719.

(15) Bodnarchuk, M. I.; Kovalenko, M. V.; Heiss, W.; Talapin, D. V. *J. Am. Chem. Soc.* **2010**, *132*, 11967.

(16) Talapin, D. V.; Lee, J. S.; Kovalenko, M. V.; Shevchenko, E. V. *Chem. Rev.* **2010**, *110*, 389.

(17) Alder, B. J.; Hoover, W. G.; Young, D. A. *J. Chem. Phys.* **1968**, *49*, 3688.

(18) Li, L.; Ismagilov, R. F. *Annu. Rev. Biophys.* **2010**, *39*, 139.

(19) Shevchenko, E.; Talapin, D.; Kornowski, A.; Wiekhorst, F.; Kotzler, J.; Haase, M.; Rogach, A.; Weller, H. *Adv. Mater.* **2002**, *14*, 287.

(20) Nagel, M.; Hickey, S. G.; Fromsdorf, A.; Kornowski, A.; Weller, H. *Z. Phys. Chem.* **2007**, *221*, 427.

(21) Shevchenko, E. V.; Talapin, D. V.; Rogach, A. L.; Kornowski, A.; Haase, M.; Weller, H. *J. Am. Chem. Soc.* **2002**, *124*, 11480.

(22) Talapin, D. V.; Shevchenko, E. V.; Kornowski, A.; Gaponik, N.; Haase, M.; Rogach, A. L.; Weller, H. *Adv. Mater.* **2001**, *13*, 1868.

(23) Cherezov, V.; Peddi, A.; Muthusubramaniam, L.; Zheng, Y. F.; Caffrey, M. *Acta Crystallogr., Sect. D* **2004**, *60*, 1795.

(24) Hansen, C. L.; Classen, S.; Berger, J. M.; Quake, S. R. *J. Am. Chem. Soc.* **2006**, *128*, 3142.

(25) Hansen, C. L.; Skordalakes, E.; Berger, J. M.; Quake, S. R. *Proc. Natl. Acad. Sci. U.S.A.* **2002**, *99*, 16531.

(26) Zheng, B.; Ismagilov, R. F. *Angew. Chem., Int. Ed.* **2005**, *44*, 2520.

(27) Zheng, B.; Roach, L. S.; Ismagilov, R. F. *J. Am. Chem. Soc.* **2003**, *125*, 11170.

(28) Tice, J. D.; Song, H.; Lyon, A. D.; Ismagilov, R. F. *Langmuir* **2003**, *19*, 9127.

(29) Li, L.; Mustafi, D.; Fu, Q.; Tereshko, V.; Chen, D. L. L.; Tice, J. D.; Ismagilov, R. F. *Proc. Natl. Acad. Sci. U.S.A.* **2006**, *103*, 19243.

(30) Lee, J. N.; Park, C.; Whitesides, G. M. *Anal. Chem.* **2003**, *75*, 6544.

(31) See the Supporting Information.

(32) Pompano, R. R.; Li, H. W.; Ismagilov, R. F. *Biophys. J.* **2008**, *95*, 1531.

(33) Bodnarchuk, M. I.; Kovalenko, M. V.; Groiss, H.; Resel, R.; Reissner, M.; Hesser, G.; Lechner, R. T.; Steiner, W.; Schaffler, F.; Heiss, W. *Small* **2009**, *5*, 2247.

(34) Hines, M. A.; Scholes, G. D. *Adv. Mater.* **2003**, *15*, 1844.

(35) Burton, W. K.; Cabrera, N.; Frank, F. C. *Philos. Trans. R. Soc. London* **1951**, *243*, 299.

(36) Bierman, M. J.; Lau, Y. K. A.; Kvit, A. V.; Schmitt, A. L.; Jin, S. *Science* **2008**, *320*, 1060.

(37) Song, H.; Tice, J. D.; Ismagilov, R. F. *Angew. Chem., Int. Ed.* **2003**, *42*, 768.

(38) Hunt, N.; Jardine, R.; Bartlett, P. *Phys. Rev. E* **2000**, *62*, 900.

(39) Kalsin, A. M.; Fialkowski, M.; Paszewski, M.; Smoukov, S. K.; Bishop, K. J. M.; Grzybowski, B. A. *Science* **2006**, *312*, 420.

(40) Ohara, P. C.; Leff, D. V.; Heath, J. R.; Gelbart, W. M. *Phys. Rev. Lett.* **1995**, *75*, 3466.

(41) Roach, L. S.; Song, H.; Ismagilov, R. F. *Anal. Chem.* **2005**, *77*, 785.

(42) Kreutz, J. E.; Li, L.; Roach, L. S.; Hatakeyama, T.; Ismagilov, R. F. *J. Am. Chem. Soc.* **2009**, *131*, 6042.